

UNRAVELLING THE ORIGIN OF ULTRALAMINAE IN SEDIMENTARY ORGANIC MATTER: THE CONTRIBUTION OF BACTERIA AND PHOTOSYNTHETIC ORGANISMS

MURIEL PACTON,¹ GEORGES E. GORIN,¹ AND NICOLAS FIET²

¹Department of Geology-Paleontology, University of Geneva, Geneva, Switzerland

²UMR-CNRS 8148, Bat. 504, Paris-Sud University, 91405 Orsay Cedex, France

ABSTRACT: Conditions for OM preservation depend on both the chemical nature of constituents and environmental factors. Among known preservation pathways, the selective preservation is based on refractory molecules such as algaenans, which are algal components. So far, ultralaminae have been considered as remains of microalgal cell walls on the basis of microscopic and organic geochemical similarities between fossil kerogen and recent algae. This high-resolution microscopic study focuses on organic matter (OM) from different fossil environments, i.e., from shallow to deep water. This OM is compared with recent organic analogs, i.e., microbial mats and biofilm, using transmission electron microscopy. Four possible origins of ultralaminae can be interpreted: algal and bacterial cell walls, thylakoids, and filamentous organisms. This highlights the importance of ultralaminae as a major indicator for paleoenvironmental interpretation. The multiple origin of ultralaminae implies new considerations about OM preservation and depositional conditions. In this way, the role of bacteria in OM accumulations can be reevaluated and the presence of ultralaminae such as thylakoids has a potential to become a new indicator of photosynthesis in fossil sediments.

INTRODUCTION

Insoluble sedimentary organic matter (SOM) from lacustrine and marine source rocks and oil shales, ranging in age from Infra-Cambrian to Miocene, contains typical lamellar structures called ultralaminae. Their morphological description has so far been very basic: they are very thin (10–30 nm) and grouped into bundles (Largeau et al. 1990; Lichtfouse et al. 1996; Raynaud et al. 1988; Raynaud et al. 1989). Ultralaminae have been shown to originate from the selective preservation of algaenans, i.e., non-hydrolyzable, highly aliphatic macromolecular constituents, which build up very thin (10–30 nm), chemically resistant outer walls in various organisms, among which green algae (Chlorophyceae) have been extensively studied (Derenne et al. 1991; Tegelaar et al. 1989). Algaenans are characterized by a conspicuous resistance to non-oxidative chemical degradation including drastic base and acid hydrolyses (Derenne and Largeau 2001).

Some single-cell algae (i.e., *Scenedesmus*, *Botryococcus braunii*, *Tetradron minimum*) possess additional outer walls containing solvent-insoluble macromolecules characterized by an unusually high resistance to chemical degradation and by a highly paraffinic structure (Berkaloff et al. 1983; Goth et al. 1988; Kadouri et al. 1988). Therefore, comparisons have been carried out between recent microalgae (Chlorophyceae), in particular *Nanochlorum eucaryotum*, *Scenedesmus crassus*, *S. armatus*, and *S. quadricauda* (Largeau et al. 1990), and fossil kerogens. Some similarities have been observed between fossil kerogens and recent algae, i.e., *Scenedesmus quadricauda*, based on biomarkers and morphology (Derenne et al. 1991; Largeau et al. 1990). Nevertheless, the comparison of *S. quadricauda* algaenans with Chlorophyceae revealed important differences in both morphology and chemical composition (Derenne et al. 1991).

From a geochemical point of view, alkyl nitriles have so far been identified only in the algaenan pyrolysates of both freshwater Chloro-

phyceae with very thin resistant outer walls and their fossil counterparts, the ultralaminae of lacustrine kerogens (Derenne et al. 1991).

Organic-rich rocks deposited in anoxic marine conditions contain large amounts of microscopically amorphous organic matter (AOM). Ultralaminae are the only visible structures in transmission electron microscopy (TEM) and point to the selective preservation pathway as a dominant process in organic matter (OM) preservation and, of course, to an algal contribution in OM formation.

So far ultralaminae have always been identified as microalgal cell walls. Moreover, fossilization of algal structures depends on the degree of OM preservation. Because chemical compounds extracted and identified through organic geochemistry reflect the whole extractable OM, it seems impossible to associate them with specific parts of such organisms, e.g., cell walls, membranes of inclusions and granules, etc. Therefore, there are still many uncertainties associated with the interpretation of ultralaminae.

The goal of this study is to investigate AOM in well-known, anoxic, fossil environments with a specific emphasis on the occurrence of ultralaminae using TEM. The chosen paleoenvironments are well documented through organic geochemistry and sedimentology. It is hoped to highlight the genetic origin of ultralaminae in order to determine the preservation state of OM and which parts of such structures are preserved. Results on fossil OM have been confirmed through comparison with recent microbial analogs, i.e., microbial mats and biofilm.

BIOLOGICAL BACKGROUND: ALGAL VS. BACTERIAL CELL WALLS AND THYLAKOID MEMBRANES

Algal Cell Walls

Algal cells may be naked or covered by either complete and rigid, or incomplete cell walls, or a series of plates, strips, or inorganic and

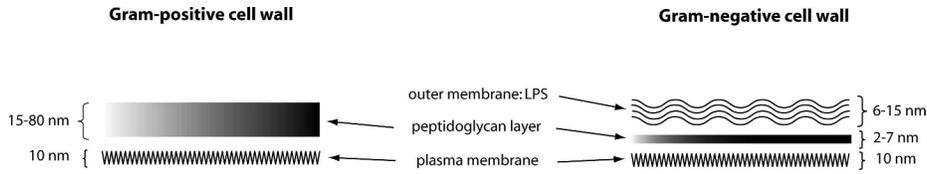


FIG. 1.—Schematic representation of bacterial cell walls showing differences between Gram-negative and Gram-positive bacteria.

sometimes organic scales. In general, cell walls comprise two constituents: an amorphous component which forms the matrix, within which the second fibrillar component is embedded (Madigan et al. 2003). The latter forms the wall rigid skeleton, and is commonly made of cellulose. The amorphous components are mainly polysaccharides.

Bacterial Cell Walls

Bacteria are classified in two classes on the basis of the composition of their cell wall (Madigan et al. 2003). The cell wall of Gram-positive bacteria is composed of several layers of peptidoglycan with a thickness ranging from 15 to 80 nm. The cell wall of Gram-negative bacteria is high in lipid content and low in peptidoglycan content. It is composed of two specific zones which surround the 10 nm thick plasma membrane: the periplasmic space and the lipopolysaccharide layer (LPS). The periplasmic space separates the outer plasma membrane from the 2–7 nm thick peptidoglycan layer. The Gram-negative cell wall is similar to a cytoplasmic membrane, typically only a few layers thick and generally much thinner than Gram-positive types (Fig. 1).

Thylakoids

Generally, thylakoids are defined as membranes where photosynthesis occurs. Their arrangement in prokaryotes and eukaryotes is different (Fig. 2). Despite many years of study, little is known about the 3D architecture of cyanobacterial thylakoid membranes.

In eukaryotes, photosynthesis is associated with special intracellular organelles, the chloroplasts. Chloroplasts have a double-membrane envelope, called the chloroplast envelope. Each membrane is a phospholipid bilayer, each one being some 6 and 8 nm thick respectively and the two separated by a gap of 10–20 nm called the intermembrane space. Within the inner membrane, in the zone called stroma, thylakoids are characterized by interconnecting flattened membrane compartments (Madigan et al. 2003). In prokaryotes, chloroplasts are absent, in contrast to eukaryotes.

METHODS

All marine rock samples studied are macroscopically characterized by organic-rich laminites. An alternation of organic and mineral layers

is clearly identified in rock thin sections. Fossil OM has been sampled in five typical black shales of different age where AOM is the dominant organic constituent: the deep-water Miocene Monterey Formation (Isaacs and Rullkötter 2001) at Naples Beach in California (Fig. 3); the Kimmeridgian bituminous shales (Bernier 1984; Tribovillard et al. 1999) at Orbagnoux in the French Jura (Fig. 4), deposited in a shallow back-reef environment; and three Cretaceous oceanic anoxic events (OAEs) in Central Italy, including the Selli level (Baudin et al. 1998), the Urbino level (Pratt and King 1986), and the 113 level (Pratt and King 1986) (Fig. 5), where depositional conditions are still debated.

Two recent bacterial analogs have been considered: a biofilm containing cyanobacteria and green algae (Silva e Silva et al. 2004), developed in a laboratory culture from a microbial mat sampled in Lagoa Vermelha, Brazil (Vasconcelos 1994); and a microbial mat sampled in hypersaline conditions at Hassi Jerbi in southern Tunisia (Davaud and Septfontaine 1995). The Hassi Jerbi mat was sampled in the field and was preserved in plastic bags in a cool box at 5°C during transport. Then it was acid etched for analyses in TEM.

The observation of fossil OM in consolidated rocks requires desintegration of the mineral fraction through a standard palynological preparation technique, in order to isolate OM. This is achieved through a HCl (30%) and HF (70%) acid treatment followed by heavy-liquid separation (Steffen and Gorin 1993). In general, 20 g were used to obtain kerogen. At the end of this treatment, the OM quantity varied from one to a few grams, depending on the total organic content of the studied rocks. The recent microbial mats studied here were also exposed to the same acid treatment for a proper comparison with fossil OM, i.e., to verify that this treatment does not introduce any artifact. Subsequently, transmission electron microscopy (TEM) was used to investigate the OM ultrastructure in ultrathin sections. For TEM observations, recent and fossil OM were fixed in 1% glutaraldehyde in 50 mM cacodylate buffer at pH 7.4 (CB) and at room temperature for one hour, washed three times in CB, and postfixed in 1% osmium tetroxyde in CB for one hour at room temperature. After three washes in CB, the material was embedded in 2.5% agarose and dehydrated before inclusion in Epon. Between four and six blocks were made for each sample. Thin sections (70 nm) were obtained using a Leica ultramicrotome and contrasted with uranyl acetate for 15 min. TEM observations

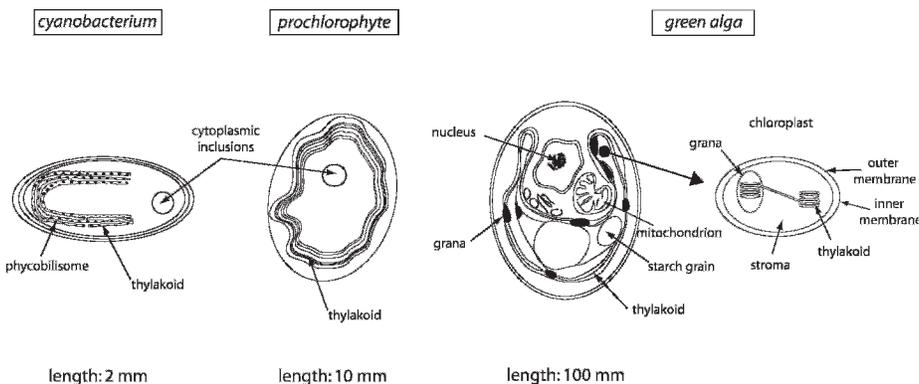


FIG. 2.—Schematic representation of thylakoid membranes in prokaryotes (cyanobacterium and prochlorophyte) and green alga.

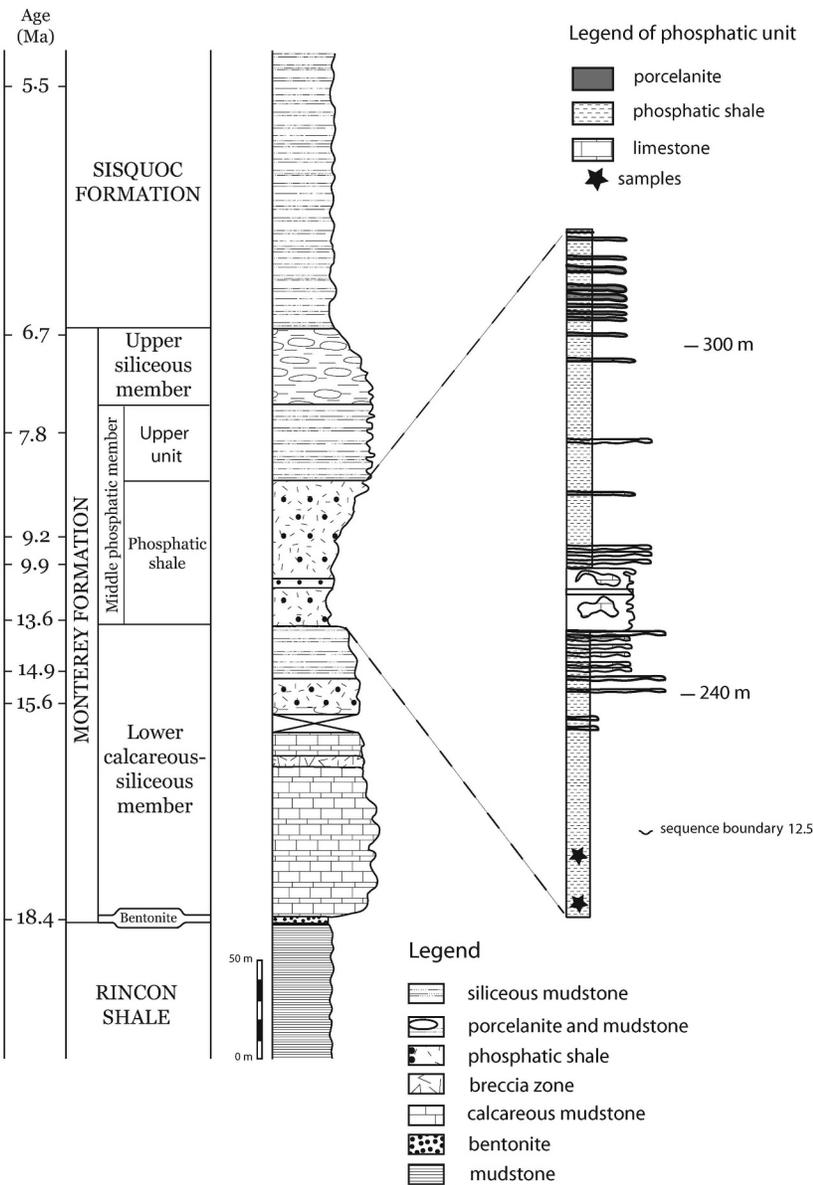
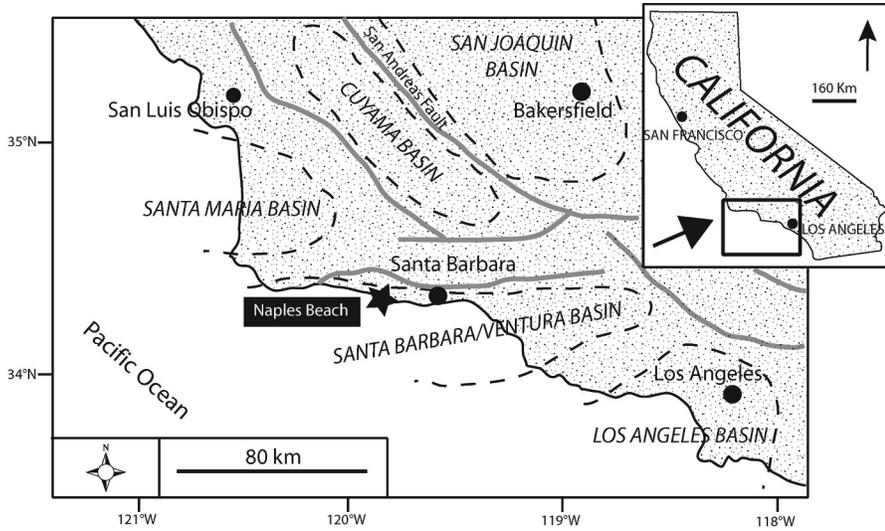


FIG. 3.—Location of the Naples Beach section in the Miocene Monterey Formation (California). Stratigraphic sequence at Naples Beach (modified after Isaacs and Rullkötter 2001).

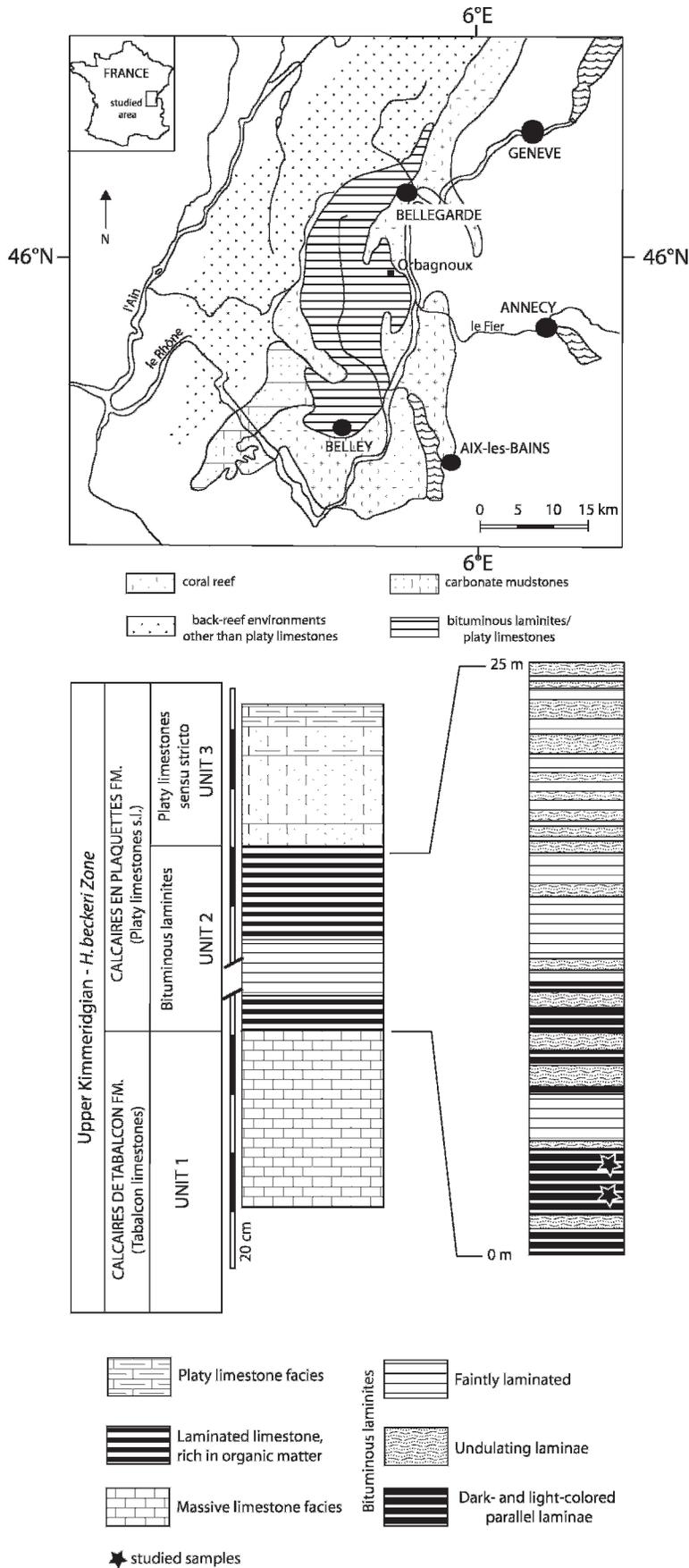
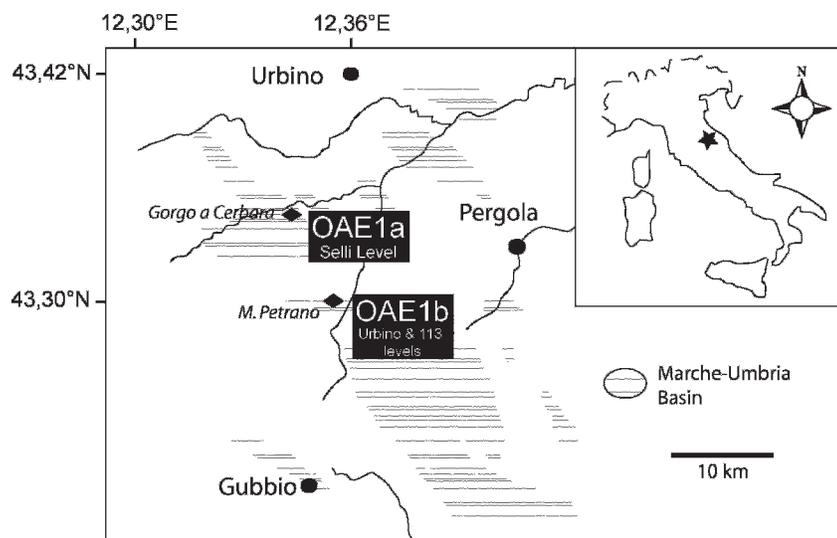


FIG. 4.—Palaeogeography of the Upper Jurassic in the southern Jura and location of the Orbagnoux section (modified after Bernier 1984) and schematic lithological column of the bituminous laminites at Orbagnoux (modified after Tribouillard et al. 2000).



Epoch	Age	Lithology	Formations	studied organic-rich marker beds
LATE CRETACEOUS	Danian	[Brick pattern]	SCAGLIA ROSSA	
	Maastrichtian			
	Campanian			
	Santonian			
	Coniacian			
	Turonian			
	Cenomanian		SCAGLIA BIANCA	
EARLY CRETACEOUS	Albian	[Horizontal lines]	MARNE A FUCOIDI	← Urbino Level (OAE1b)
	Aptian			← 113 Level (OAE1b)
	Barremian			← Selli Level (OAE1a)
	Hauterivian			
	Valanginian		MAIOLICA	
	Berriasian			
MALM	Tithonian			

FIG. 5.—Location map of OAEs studied in the Marche-Umbria Basin (Central Italy). Stratigraphic columns of OAE1a and OAE1b (modified from (Cocconi et al. 1989).

were performed with a Phillips CM100 transmission electron microscope (Paris-Sud University), and digital image processing was applied. Four different areas in each sample were studied using some 50 ultrathin sections in order to have a representative estimation of observed structures. The proportion of ultralaminiae in OM was visually evaluated.

RESULTS AND DISCUSSION

TEM observations showed heterogeneous material characterized by amorphous matter, bacteria, EPS, and ultralaminiae. Ultralaminiae were rare in the Monterey Formation (< 1% of OM) but abundant in the Kimmeridgian laminites (40% of OM) and in the OAEs (50% of OM).

TABLE 1.—Summary of the main characteristics shown by the form types of ultralaminae distinguished in fossil OM.

characteristics	algal cell walls	bacterial cell walls	thylakoids	organisms
thickness	commonly 100–150 nm; rarely 35 nm	variable: 30–150 nm	35–60 nm	120–150 nm
appearance	patch-forming; contorted, elongated spirals or linear with granule layers	linear or contorted layers	linear or randomly distributed contorted string-like layers: stacked, sometimes stacked by pair (cyanobacteria)	complex organization with outer membrane and inner content
texture	dense and homogeneous with sharp outlines	ill- to well-defined, blurred; sometimes dense	sharp outlines	heterogeneous
length	10 μm	several μm	several μm	> 10 μm
degradation	rarely diffuse; radially fragmented	burst	sometimes fragmented	not observed

The recognition of four different types of structures in ultralaminae has three major implications for OM study, i.e., OM origin, OM preservation conditions and paleobathymetry.

Recognition of the Different Types of Ultralaminae in Fossil and Recent Material

Comparison of recent laminar ultrastructures with similar structures in SOM reveals different types of ultralaminae: algal cell walls, bacterial cell walls, thylakoid membranes, and organisms on their own. Based on microscopic observations, the specific characteristics of each class (especially width, texture, and degradation aspect) can be specifically determined (Table 1):

Algal Cell Walls.—Algal cell walls are commonly 100–200 nm thick and have a particularly dense and homogeneous texture. In both recent and fossil material, outlines are sharp. They occur as elongated spirals or contorted layers associated with small granules, which can be inclusions and granules serving as specific storage sites (Konhauser 2007). Their length of about 10 μm is significant. When they are degraded, they appear as layers locally diffuse, and in some cases a radial fragmentation is observed.

In the recent biofilm, algae resembling green algae associated with the class Chlorophyceae showed some layers 100 nm thick (Fig. 6A). After acid etching, no entire algal cell was observed. Only dense layers sometimes characterized by diffuse outlines were preserved, the thickness of which ranges from 80 to 170 nm (Fig. 6B).

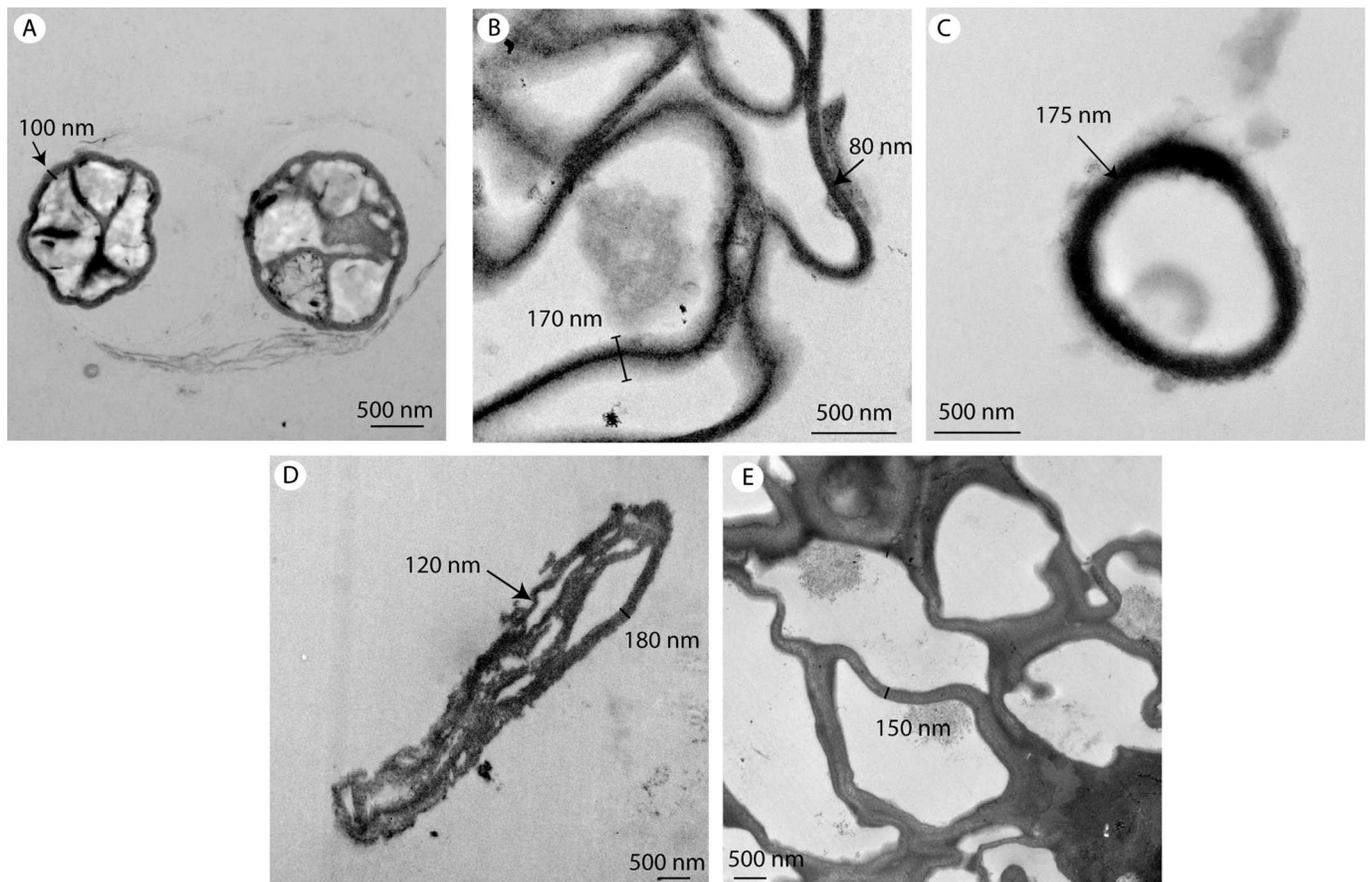


FIG. 6.—Transmission electron microscopy (TEM) sections showing recent algal cell walls: A) in the biofilm (Chlorophyte genus); B) in the biofilm after acid etching; C, D) in the microbial mat of Hassi Jerbi (southern Tunisia) after acid etching; E) *Botryococcus braunii* after acid etching. See text for description.

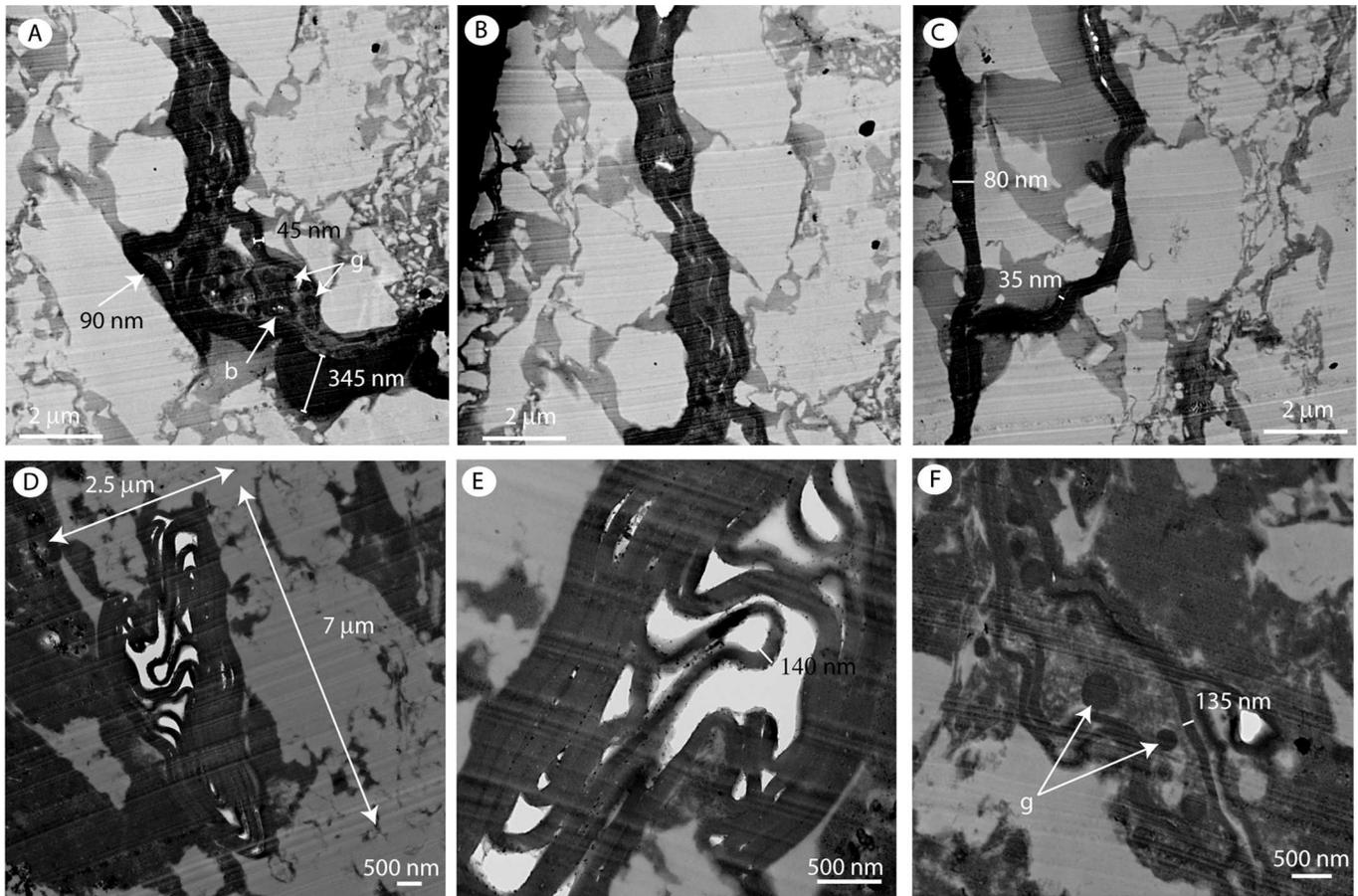


FIG. 7.—TEM sections showing fossil algal cell walls: A) associated with granules (g) and symbiotic bacteria (b) in Kimmeridgian laminites; B) long linear layers in Kimmeridgian laminites; C) arrangement similar to *Botryococcus braunii* in Kimmeridgian laminites; D, E) contorted layers in the Selli level; F) layers associated with granules (g) in the Selli level. See text for description.

Similar, dense concentric layers 175 nm thick were found in the recent microbial mat of Hassi Jerbi (Fig. 6C). Sometimes, they appeared as contorted layers with “sharp” outlines and a thickness ranging from 120 to 180 nm (Fig. 6D).

Fossil OM in Kimmeridgian laminites contained these same layers, which locally widen and sometimes were spread out (Fig. 7A); their thickness ranged from 45 to 90 nm on average, with a maximum of 350 nm. They surrounded a patch constituted of small dark granules, assimilated to inclusions or granules and rod-shaped cellular forms, which are typical of bacteria. Therefore, these structures are reminiscent of algae with symbiotic bacteria. They could form structures more than 10 μm long (Fig. 7B). Layers had the same appearance as those formed in recent microbial mats and ranged in thickness from 35 to 80 nm (Fig. 7C). Their arrangement was similar to that in *Botryococcus braunii* (Fig. 6D).

In the Selli level, fossil OM showed a concentric arrangement of layers, sometimes forming patches up to 7 μm \times 2.5 μm in size (Fig. 7D). Layers had sharp edges with sometimes diffuse, blurred substances inbetween the pigmentation (Fig. 7E). They appeared as contorted layers surrounding a zone with some granules (Fig. 7F). Some were 135 nm thick and resembled those in figure 7A.

In the 113 level, similar contorted layers formed extensive patches (Fig. 8A). At high magnification, layers appeared stacked by pairs, which were some 245 nm thick and radially fragmented (Fig. 8B). This arrangement was similar to that in figure 7E, although the fragmented

appearance suggested a degraded state. Single layers 60 to 150 nm thick, and sometimes broken or spread out, were also observed (Fig. 8C).

Fossil OM in the Urbino level contained a 6 μm \times 2 μm patch composed of elongated, contorted, well defined layers, up to 150 nm thick (Fig. 8D), which were similar to those of figures 7D and 8A.

Fossil OM in the Monterey Formation showed some 145 nm thick layers, which were sometimes diffuse, with a streamer-like form (Fig. 8E). They were considered to be degraded ultralaminiae.

Bacterial Cell Walls.—Bacterial cell walls were characterized by a wide size range (50–150 nm), depending on the nature of the cell wall (Gram-negative or Gram-positive bacteria). The texture was heterogeneous, and dense or translucent. No significant difference in the arrangement, size, and density was observed between fossil and recent bacteria. The length was not a significant parameter because some filamentous bacteria could be several micrometers long. They occurred as single or contorted layers but could be differentiated from algal cell walls through their more diffuse aspect. The thin or burst parts were interpreted as resulting from the degradation of bacterial cell walls both in recent bacteria and fossil OM.

In the recent biofilm, typical cyanobacteria (Fig. 9A) were characterized by a Gram-negative cell wall showing the following constituents: an undulating, outer membrane 13 nm thick; a dense layer, 4.5 nm thick, with sharp outlines, assimilated to the peptidoglycan layer; and a diffuse, layer 14 nm thick, showing the same contrast as the outer membrane, typical of the plasma membrane. The total thickness of the cell wall was

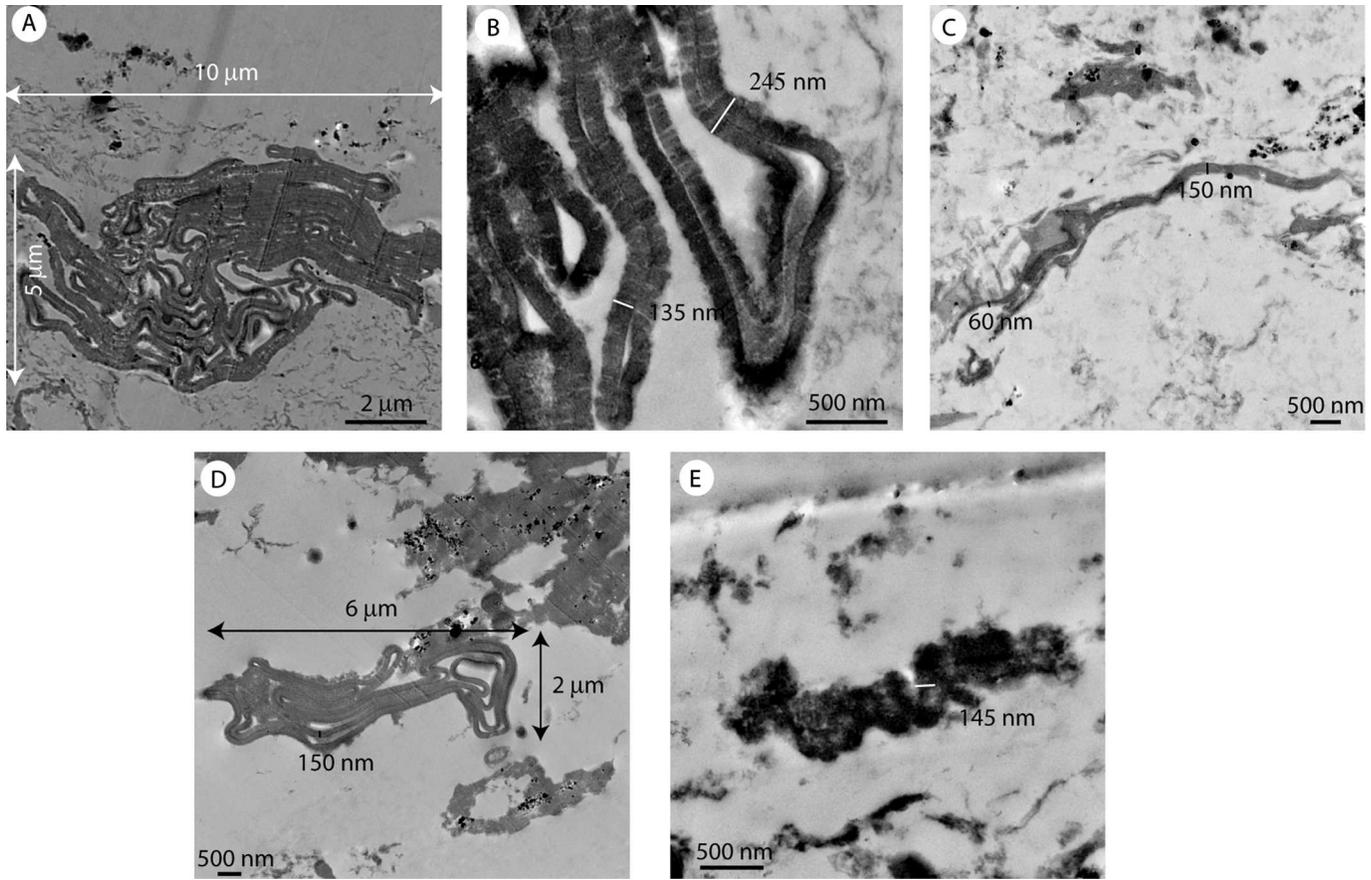


FIG. 8.—TEM sections showing fossil algal cell walls: A) extensive patch of contorted layers in the 113 level; B) amplification of contorted layers showing a radial fragmentation layers in the 113 level; C) linear layers in the 113 level; D) patch of contorted layers in the Urbino level; E) degraded contorted layers in the Monterey Formation. See text for description.

57 nm. After acid etching, only the peptidoglycan layer and the outer membrane were preserved, with a total thickness of 140 nm (Fig. 9B). This cell wall could be fossilized through diagenesis because LPS (composing Gram-negative bacteria) were more resistant to degradation than peptidoglycan (major component in Gram-positive bacteria).

The recent microbial mat of Hassi Jerbi exhibited some 500 to 900 nm thick, filamentous forms, which were less contrasted (Fig. 9c) than forms observed in algal walls (e.g., Fig. 6d). They appeared not well preserved but could be ascribed to filamentous bacteria. Finally, a mixture of different layers with variable thicknesses could be observed (Fig. 9d): when thick (up to 155 nm), their aspect was translucent; when thin, layers were dense and dark, with a thickness ranging from 15 to 50 nm.

Fossil OM in Kimmeridgian laminites showed a mixture of different types of membranes with variable thicknesses (Fig. 10a). Translucent layers were 60 nm thick and homogeneous, whereas dense layers ranged in thicknesses from 50 to 140 nm. Their aspect was similar to that of layers in figure 9d, and indicated a certain stage of degradation.

Fossil OM in the Selli level displayed diffuse layers, sometimes stacked with dark-coloured boundaries (Fig. 10b). One was 30 nm thick and the total thickness of the stack ranged from 155 to 330 nm. This probably indicated a certain degradation stage, but different from that in figure 9d. It was maybe specific to the composition of the ultralaminae or due to different degradation conditions prior to diagenesis.

Fossil OM in the 113 level showed relatively dark, contrasted, contorted, 70 nm thick layers (Fig. 10c).

Fossil OM in the Urbino level contained contorted dark layers with an average thickness of 30 nm, separated by a weakly contrasted and diffuse zone (Fig. 10d).

Fossil OM in the Monterey Formation displayed dark layers with well defined or diffuse outlines (Figs. 10e & 10f). They were stacked, with thicknesses ranging from 85 to 100 nm. When they had burst, they appeared diffuse, and up to 300 nm thick.

Thylakoid Membranes.—Thylakoid membranes are typically thin layers, ranging from 35 to 70 nm in thickness. Another important parameter is their occurrence: they are grouped by pairs or stacked, depending on the cyanobacterial or algal origin. Their outline is generally sharp, but their internal texture is not always dense. Their length is variable because of the form of organisms (filamentous, coccoid, or bacillus). No change was observed in the recent material after the acid treatment. In fossil OM, they can be fragmented.

In the recent biofilm, cyanobacterial thylakoids appeared as homogeneous, 70 nm thick membrane pairs, which were parallel to the cell (Fig. 11A). They were placed side by side, possessed sharp outlines, and contained small dark grains resembling phycobilisomes. The space between each membrane was constant and some 30 nm thick. Thylakoids could sometimes present a diffuse aspect, but their thickness was smaller, 35 nm (Fig. 9A).

The recent biofilm also contained algae where thylakoid membranes were randomly placed in the cell (Fig. 11B). They were 40 nm thick and locally stacked to each other (i.e., grana). The same distribution was

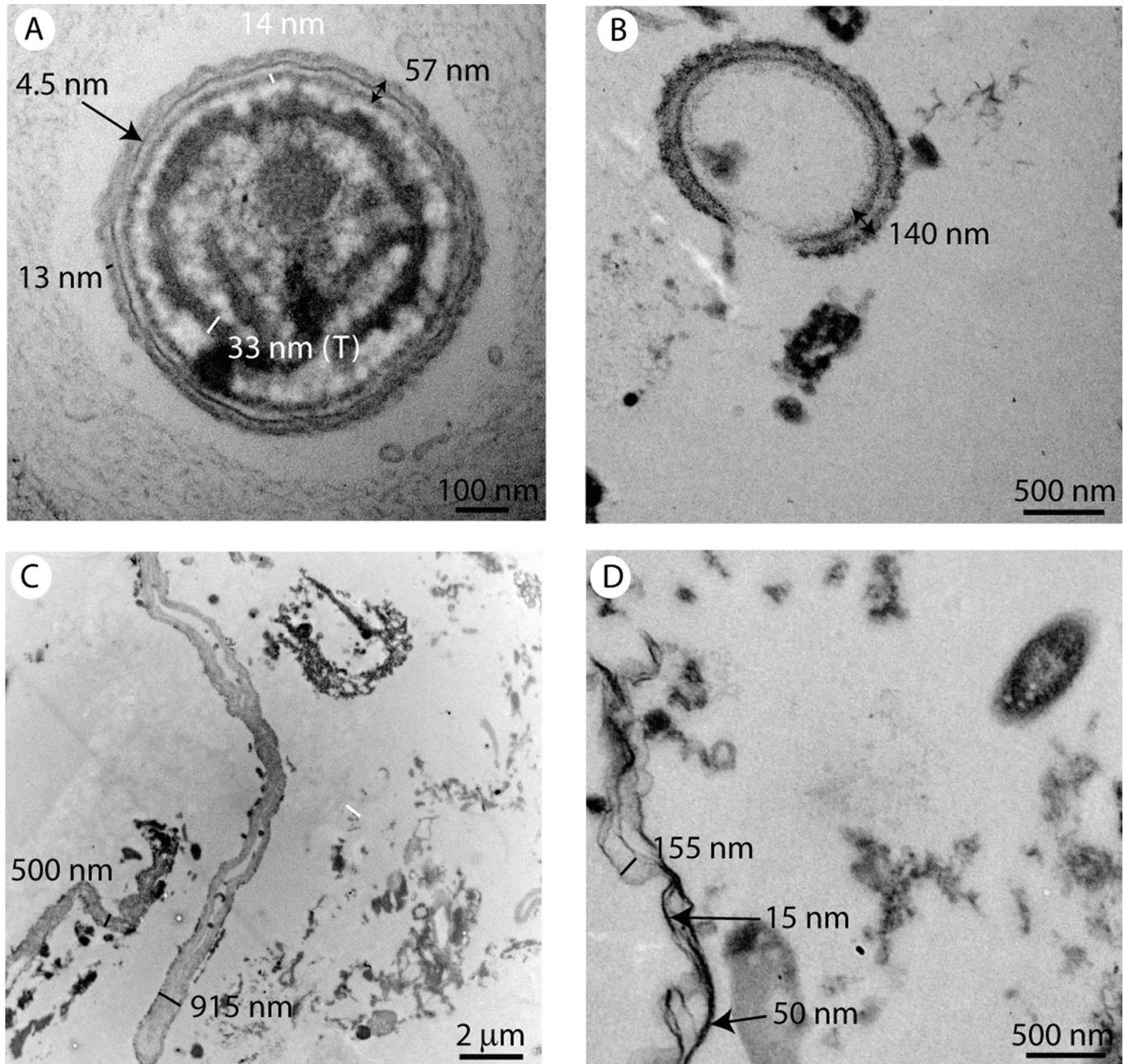


FIG. 9.—TEM sections showing recent bacterial cell walls: A) Gram-negative cell wall of cyanobacteria in the biofilm; B) same Gram-negative cell wall in the biofilm after acid etching; C) remnants of filamentous bacteria in the Hassi Jerbi microbial mat after acid etching; D) burst translucent layers attached to dense thin membranes in the Hassi Jerbi microbial mat after acid etching. See text for description.

observed in other algal species where thylakoids were about 50 nm thick and locally stacked in grana (Figs. 11C,D). After acid etching, these membranes were denser but with a similar size (60 nm), with some cytoplasmic inclusions (Fig. 11E).

Thylakoids in fossil OM of Kimmeridgian laminites were characterized by a succession of light-colored layers, 80 nm thick, stacked by pairs and dark-colored laminae 300 nm thick (Fig. 12A). Each light layer was 40 nm thick. The arrangement was generally regular, sometimes undulated (Pacton et al. 2006).

Fossil OM in the Selli level displayed ill-defined, dark, parallel, 60 nm thick layers in a less contrasted patch (Fig. 12B). This arrangement could be related to degraded material.

Fossil OM in the 113 level displayed a patch of diffuse layers, sometimes discontinuous and undulating. The layer thickness was about 35 nm (Fig. 12C).

In the Urbino level, a sequence of contorted, dark-colored, 20 nm thick, paired layers separated by light-colored intervals was observed. Layers had a sharp outline (Fig. 12D).

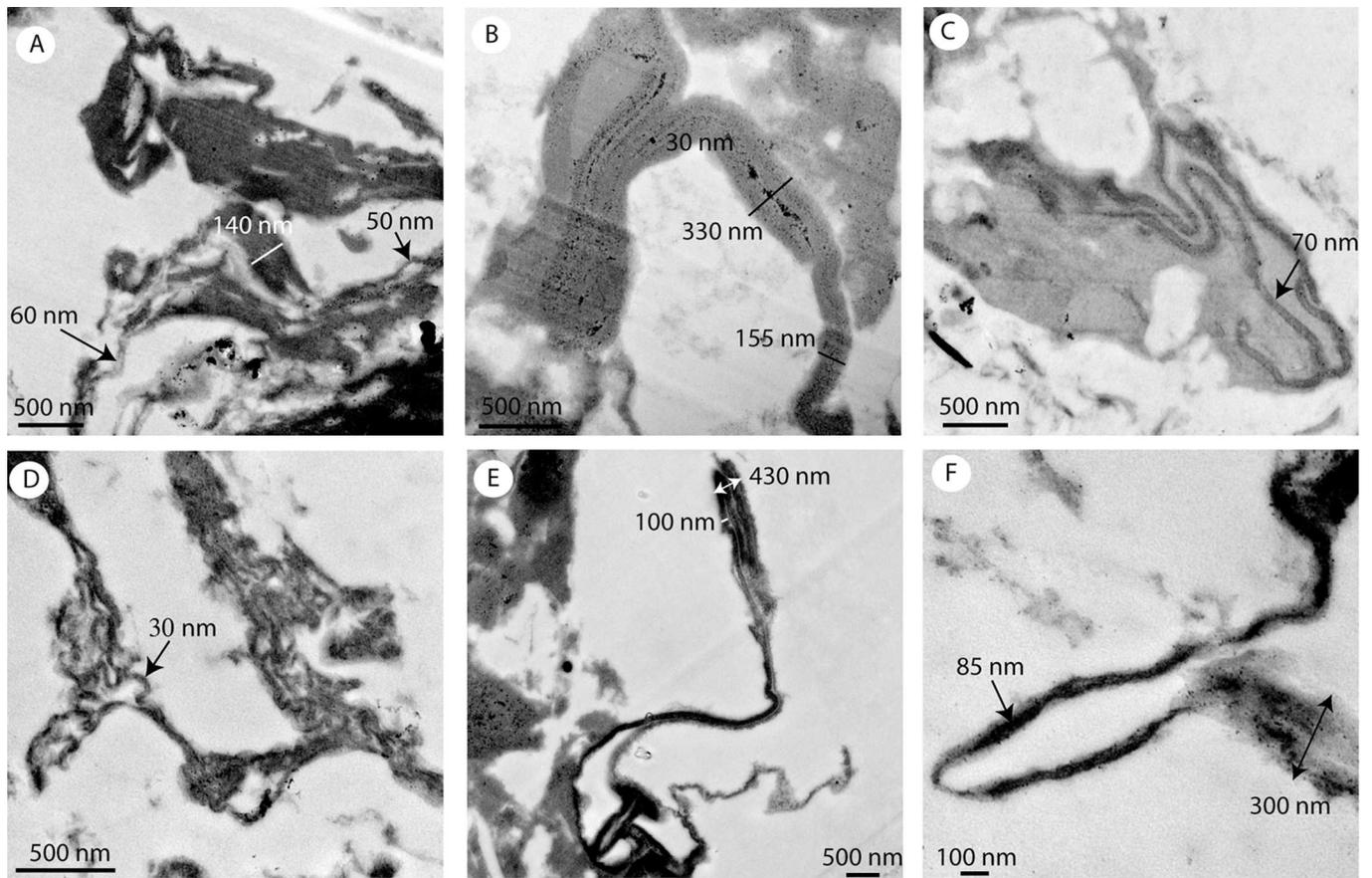


FIG. 10.—TEM sections showing fossil bacterial cell walls: A) mixture of cell walls in Kimmeridgian laminites; B) more or less diffuse contorted layers in the Selli level; C) contorted layers in a diffuse mass in the 113 level; D) thin contorted layers in the Urbino level; E, F) dense, locally burst layer in the Monterey Formation. See text for description.

Organisms and Others.—Organisms on their own were characterized by a typical thick membrane separated from an internal cell. The occurrence of such well-preserved structures was rare because most of the time only cell walls were observed. If degraded, they could be mixed up with the classes cited above. They were differentiated from simple cell walls because of their complex constitution including outer membranes. They were architecturally too evolved to be cell walls similar to those previously described.

The recent Hassi Jerbi microbial mat contained a smaller amount of dense contorted forms of variable thickness (180 nm on average). This may be due to degradation or because they were less present initially (Fig. 13A). Their aspect could not be related to algal or bacterial structures, but may be ascribed to plants, and more specifically to fossil cuticles, which show the sinuous lamellae in lower epidermis zone (Taylor 1999).

Lamellar structures were found in fossil OM of the Urbino level, but no relation could be established with the previously described structures. They appeared as filamentous, stacked, forms, more than 5 μm long, and surrounded by a typical layer resembling cell wall (Fig. 13B). This 75 nm thick layer was radially fragmented (Fig. 13C). When broken, they appeared as more translucent, twisted membranes. Filaments contained some granules and were surrounded by a more contrasted thin wall. The thickness of filaments was 120 nm, whereas that of stacked filament walls was 25 nm.

Consequently, the major distinction between cell walls and thylakoids was based on their thickness and their appearance. Cell walls appeared as thick, contorted layers, whereas thylakoids could be defined as thin layers, often grouped in pairs or stacked.

Preservation Potential of the Different Types of Ultralaminae

In the OM of all the studied fossil environments, algal and bacterial cell walls are more common than thylakoids. The latter seemed to be more affected by degradation (Fig. 14). Bacterial cell walls can be better preserved than thylakoids because of their lipid content (more abundant in Gram-negative bacteria), but they are more sensitive to degradation than algal cell walls. Thylakoids associated with photosynthetic pigments can be preserved because, although they are rich in degradable proteins, they contain a small amount of lipids. In some cases, this preservation may be due to encapsulation. This process is based on intrinsically reactive biochemical compounds encapsulated in some protective matrix (Eglinton 1998; Knicker et al. 1996). The preservation of these specific membranes, separated from other cellular components such as cell wall and storage inclusions, could be the result of separation during OM isolation treatment and/or lysis.

The resistance to degradation of each class of ultralaminae is closely related to their chemical nature.

Relation between Ultralaminae and OM Preservation Pathways

There are four known OM preservation pathways: (1) The degradation-recondensation (or recondensation) pathway is characterized by the absence of source organism morphological features. This model is based on a diagenetic fragmentation of the OM biomacromolecules (Tissot and Welte 1984). (2) The selective preservation pathway is based on the

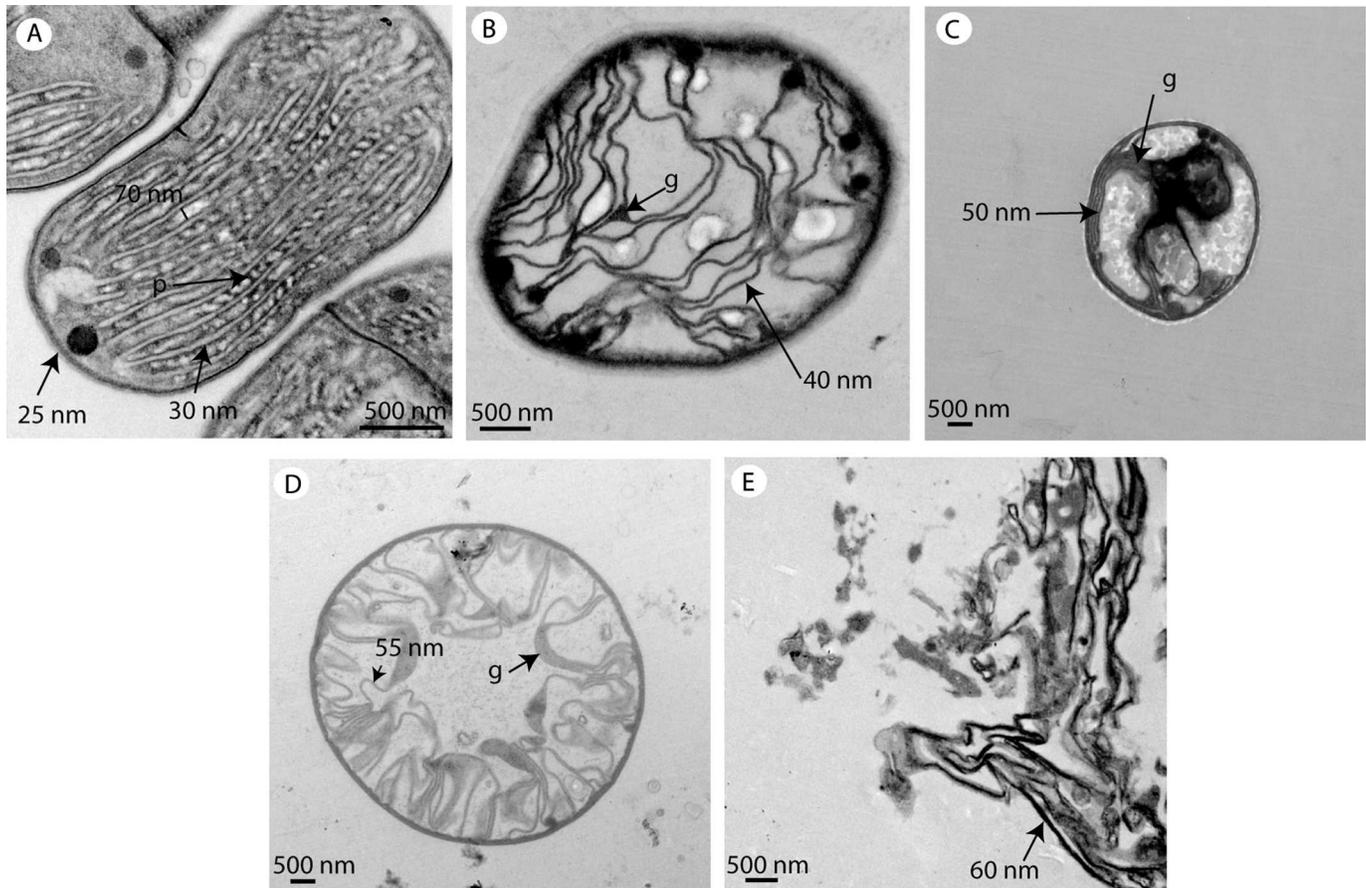


FIG. 11.—TEM sections showing recent thylakoid membranes: A) presence of phycobilisomes (p, dark) in a cyanobacterium within the biofilm; B, C, D) thylakoids assembled in grana in different species of algae within the biofilm; E) thylakoids associated with granules in the biofilm after acid etching. See text for description.

production by some living organisms, especially microalgae, of insoluble biomacromolecules highly resistant to chemical and microbial degradation. These biomacromolecules are not affected by strong basic and acid hydrolyses and also show a high resistance to microbial attacks (Goth et al., 1988; Tegelaar et al., 1989; Largeau et al., 1990). (3) The natural vulcanization is an intermolecular incorporation of inorganic sulphur species into low-molecular-weight functionalized lipids resulting in the formation of high-molecular-weight sedimentary OM (Adam et al. 1993; Kohnen et al. 1991; Sinningh  Damst  et al. 1989; Sinningh  Damst  et al. 1988). (4) The sorptive protection pathway emphasizes the protective role of minerals and/or EPS (Pacton et al. 2007; Salmon et al. 2000). This study shows a variety of ultralaminae, which cannot be distinguished in biomarker studies. Until now ultralaminae were solely associated with pyrolysates of algaenans, i.e., alkylnitriles, and therefore reflecting the role of the selective preservation pathway. Nevertheless such a chemical signature could also occur from condensation of lipids, which would mean that the role of algaenans might be overstated (Gupta et al. 2007). In the five studied environments, the degradation stage of ultralaminae is closely associated to OM preservation processes (Fig. 14). In the lower part of Figure 14, the weak degradation of OM is related to the sorptive preservation pathway (Pacton et al. 2007a), because of the labile nature of thylakoid compounds. It automatically implies the concomitant contribution of the selective preservation pathway because algae are not subjected to hydrolysis. The evolution towards degraded ultralaminae implies an increasing contribution of the degradation-recondensation pathway. According to microscopic observations, it coincides with degraded OM.

Paleoenvironmental Significance of Ultralaminae

Fossil ultralaminae such as cell walls are indicative of the selective OM preservation pathway. Refractory molecules (e.g., algaenans) mean the same in organic geochemistry. However, thylakoids cannot be identified through organic geochemistry, whereas they can be clearly identified in microscopy. More importantly, thylakoids cannot be related only to the selective OM preservation pathway. Moreover, in most sedimentary basins photosynthetic organisms living in the photic zone (0–200 m) are rapidly degraded in the water column after death. These allochthonous thylakoids would have been degraded during transport. Because they are prone to chemical and physical degradation, their presence in sediments implies exceptional preservation conditions, in places where degradation reactions are reduced, as is the case in EPS (Pacton et al. 2007). Consequently, thylakoids give information on water depth, because they were fossilized in the place where they lived, i.e., at the sea bottom. Although the different types of ultralaminae highlight the evidence of a relative proportion of eukaryotic and prokaryotic organisms, thylakoids have the potential to become an indicator of paleobathymetry.

CONCLUSIONS

Ultralaminae are typical, 10–30 nm thick lamellar structures encountered in fossil SOM. So far, they have been associated with microalgal cell walls with highly resistant, algaenan compounds. Their pyrolysates, i.e., alkylnitriles, are the evidence of the OM selective preservation pathway. Comparison of fossil ultralaminae with recent microbial analogs,

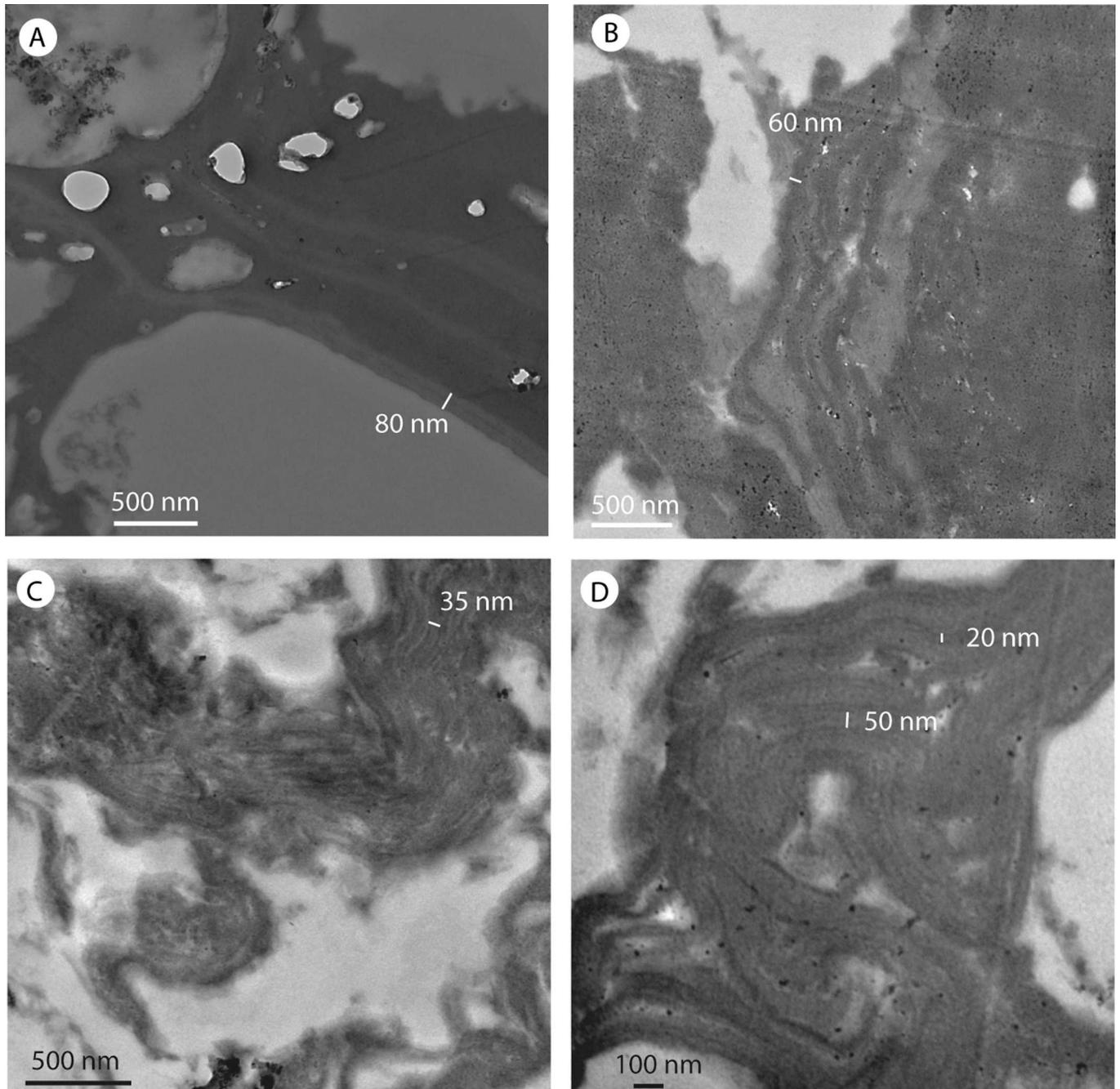


FIG. 12.—TEM sections showing fossil thylakoid membranes: A) pair of thylakoids alternating with dark zones in the kimmeridgian laminites; B) several thin layers in the Selli level; C) discontinuous, contorted lines in the 113 level; D) contorted pair of layers in the Urbino level. See text for description.

containing green algae and cyanobacteria, sheds new light on their possible multiple origin. Four classes have been identified in fossil OM:

- (1) Algal cell walls are characterized by dense layers, 100–200 nm thick, chemically composed of algaenans.
- (2) Bacterial cell walls with layers, 60–150 nm thick which have a more heterogeneous texture. They are composed of phospholipids and proteins and, in the case of Gram-negative bacteria, of lipopolysaccharides.
- (3) Thylakoid membranes are typically thin: they form string-like layers, 35–70 nm thick, which appear stacked or in pairs. They are
- (4) composed of proteins and lipids. They are associated with photosynthetic pigments which can be preserved or not, depending on their nature.
- (4) Filamentous organisms can be distinguished from the others categories through their typical cell wall.

Consequently, ultralaminae have a potential to become a new indicator, besides organic geochemistry and optical microscopy, for identifying the paleoenvironment and preservation pathways of SOM. The multiple origin of ultralaminae implies new considerations about OM preservation and depositional conditions. In particular, the ultralaminae

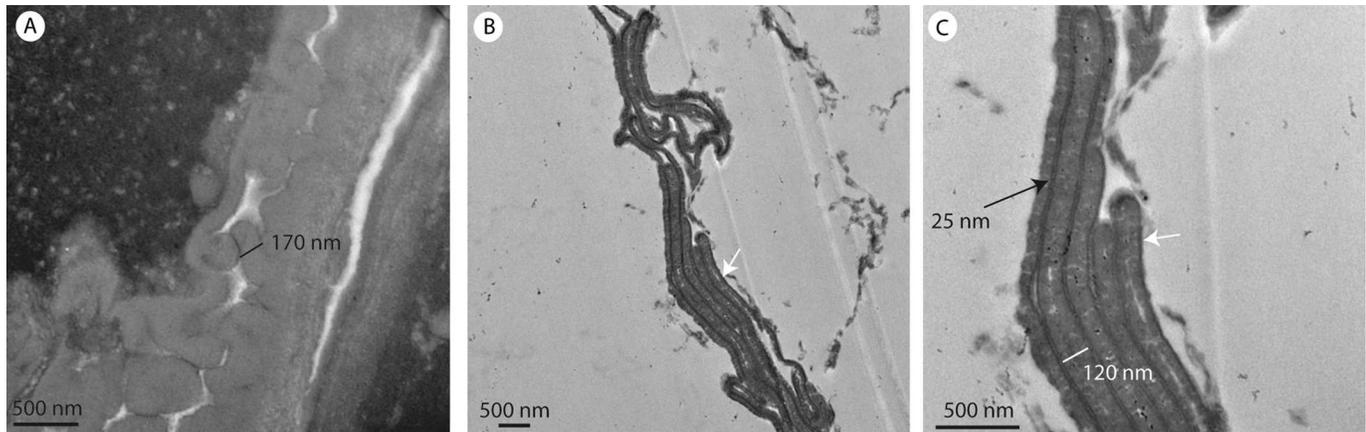


FIG. 13.—TEM sections showing other classes of ultralaminar: A) contorted layers in the Hassi Jerbi microbial mat after acid etching; B, C) stacked filamentous bodies surrounded by a typical layer in the Urbino level. See text for description.

Degradation scale of UL.	Degree of OM degradation	Degradation level of different UL types	Dominant OM preservation pathway	Examples of fossil environments
degraded	advanced		degradation-recondensation	Monterey Fm.
partially degraded	intermediate		selective preservation	L113 level Selli level
intact	weak		sorptive preservation	Orbagnoux Urbino level
		algal cell walls bacterial cell walls thylakoids organisms		

FIG. 14.—Degradation level of different ultralaminar types with respect to degree of OM degradation and dominant OM preservation pathways.

scale of degradation can be associated with the degree of OM degradation and the dominant OM preservation pathway.

Therefore, the composition of OM can be reevaluated, and ultralaminar such as thylakoids have a potential to become a new indicator of photosynthesis in fossil sediments. This has a considerable implication on the paleobathymetry which becomes restricted to the photic zone.

ACKNOWLEDGMENTS

This study is supported by the Swiss National Science Foundation (grants no. 2000.68091 and 2000.112320) and by the UMR-CNRS 8148 I.D.E.S (France), Paris-Sud. The authors thank Jeril Degrouard and Danielle Jaillard (Service Laboratory for Electron Microscopy, Department of Cellular Biology, Paris-Sud University, France) for their assistance with TEM imaging and ultramicrotome. The authors are indebted to two anonymous reviewers for their highly constructive comments.

REFERENCES

- ADAM, P., SCHMID, J.C., MYCKE, B., STRAZIELLE, C., CONNAN, J., HUC, A., RIVA, A., AND ALBRECHT, P., 1993, Structural investigation of nonpolar sulphur macromolecules in petroleum: *Geochimica et Cosmochimica Acta*, v. 57, p. 3395–3419.
- BAUDIN, F., FIET, N., COCCIONI, R., AND GALEOTTI, S., 1998, Organic matter characterisation of the Selli Level (Umbria-Marche Basin, central Italy): *Cretaceous Research*, v. 19, p. 701–714.
- BERKALOFF, C., CASADEVALL, E., LARGEAU, C., METZGER, P., PERACCA, S., AND VIRLET, J., 1983, The resistant polymer of the walls of the hydrocarbon-rich algae *Botryococcus braunii*: *Phytochemistry*, v. 22, p. 389–397.
- BERNIER, P., 1984, Les formations carbonatées du Kimméridgien et du Portlandien dans le Jura méridional. Stratigraphie, micropaléontologie et sédimentologie, Documents des Laboratoires de Géologie de Lyon, 803 p.
- COCCIONI, R., FRANCHI, R., NESCI, O., PERILLI, N., WEZEL, F., AND BATTISTINI, F., 1989, Stratigrafia, micropaléontologia e mineralogia delle Marne a Fucoidi (Aptiano inferiore-Albiano superiore) delle sezioni di Poggio le Guaine e del fiume Bosso (Appennino umbro-marchigiano): *Fossili, Evoluzione, Ambiente, Secondo Convegno Internazionale: Pergola, Italy, Atti*, p. 163–201.

- DAVAUD, E., AND SEPTFONTAINE, M., 1995, Post-mortem onshore transportation of epiphytic foraminifera: recent example from the Tunisian coastline.: *Journal of Sedimentary Research*, v. A65, p. 136–142.
- DERENNE, S., AND LARGEAU, C., 2001, A review of some important families of refractory macromolecules: composition, origin, and fate in soils and sediments: *Soil Science*, v. 166, p. 833–847.
- DERENNE, S., LARGEAU, C., CASADEVALL, E., BERKALOFF, C., AND ROUSSEAU, B., 1991, Chemical evidence of kerogen formation in source rocks and oil shales via selective preservation of thin resistant outer walls of microalgae: origin of ultralaminae: *Geochimica et Cosmochimica Acta*, v. 55, p. 1041–1050.
- EGLINTON, G., 1998, The archaeological and geological fate of biomolecules, in *Digging for Pathogens: ancient emerging diseases - their evolutionary, anthropological, and archaeological context*, Greenblatt, C.L., ed., Balaban Publishers Rehovot: Israel, p. 299–327.
- GOTH, K., DE LEEUW, J.W., PÜTTMANN, W., AND TEGELAAR, E.W., 1988, Origin of the Messel oil shale kerogen: *Nature*, v. 336, p. 759–761.
- GUPTA, N.S., MICHELS, R., BRIGGS, D.E.G., COLLINSON, M.E., EVERSHED, R.P., AND PANCOST, R.D., 2007, Experimental evidence for the formation of geomacromolecules from plant leaf lipids: *Organic Geochemistry*, v. 38, p. 28–36.
- ISAACS, C.M., AND RULLKÖTTER, J., 2001, *The Monterey Formation: From Rocks to Molecules*: New York, Columbia University Press, 553 p.
- KADOURI, A., DERENNE, S., LARGEAU, C., CASADEVALL, E., AND BERKALOFF, C., 1988, Resistant biopolymer in the outer walls of *Botryococcus braunii*, B race: *Phytochemistry*, v. 27, p. 551–557.
- KNICKER, H., SCARONI, A.W., AND HATCHER, P.G., 1996, ^{13}C and ^{15}N NMR spectroscopic investigation on the formation of fossil algal residues.: *Organic Geochemistry*, v. 24, p. 661–669.
- KOHNE, M.E.L., SINNINGHÉ DAMSTÉ, J.S., AND DE LEEUW, J.W., 1991, Biases from natural sulphurization in palaeoenvironmental reconstruction based on hydrocarbon biomarker distributions: *Nature*, v. 349, p. 775–778.
- KONHAUSER, K., 2007, *Introduction to Geomicrobiology*: Blackwell Publishing.
- LARGEAU, C., DERENNE, S., CLAIRAY, C., CASADEVALL, E., RAYNAUD, J.F., LUGARDON, B., BERKALOFF, C., COROLLEUR, M., AND ROUSSEAU, B., 1990, Characterization of various kerogens by scanning electron microscopy (SEM) and transmission electron microscopy (TEM) - Morphological relationships with resistant outer walls in extant micro-organisms: *Mededelingen. Rijks Geologische Dienst*, v. 45, p. 91–101.
- LICHTFOUSE, E., CHENU, C., AND BAUDIN, F., 1996, Resistant ultralaminae in soils: *Organic Geochemistry*, v. 25, p. 263–265.
- MADIGAN, M.T., MARTINKO, J.M., AND PARKER, J., 2003, *Biology of Microorganisms*: Columbia, Prentice Hall Publisher, 1019 p.
- PACTON, M., FIET, N., AND GORIN, G., 2006, Revisiting amorphous organic matter in Kimmeridgian laminites: what is the role of the vulcanization process in the amorphization of organic matter?: *Terra Nova*, v. 18, p. 380–387.
- PACTON, M., FIET, N., AND GORIN, G., 2007, Bacterial activity and preservation of sedimentary organic matter: the role of exopolymeric substances: *Geomicrobiology journal*, v. 24, p. 571–581.
- PRATT, L.M., AND KING, J.D., 1986, Variable marine productivity and high eolian input recorded by rhythmic black shales in Mid-Cretaceous pelagic deposits from central Italy: *Palaeoceanography*, v. 1, p. 507–522.
- RAYNAUD, J.F., LUGARDON, B., AND LACRAMPE-COULOUME, G., 1988, Observation de membranes fossiles dans la matière organique " amorphe " de roches mères de pétrole: *Compte Rendu de l'Académie des Sciences de Paris*, v. 307, p. 1703–1709.
- RAYNAUD, J.F., LUGARDON, B., AND LACRAMPE-COULOUME, G., 1989, Structures lamellaires et bactériennes, composants essentiels de la matière organique amorphe des roches mères: *Société Nationale Elf Aquitaine*, v. 13, p. 1–21.
- SALMON, V., DERENNE, S., LALLIER-VERGES, E., LARGEAU, C., AND BEAUDOIN, B., 2000, Protection of organic matter by mineral matrix in a Cenomanian black shale: *Organic Geochemistry*, v. 31, p. 463–474.
- SILVA E SILVA, L.H., SENRA, M.C.E., FARUOLO, T.C.L.M., CARVALHAL, S.B.V., ALVES, S.A.P.M.N., DAMAZIO, C.M., SHIMIZU, V.T.A., SANTOS, R.C., AND IESPA, A.A.C., 2004, Composição paleobiológica e tipos morfológicos das construções estromatolíticas da lagoa Vermelha, RJ, Brasil: *Revista Brasileira de Paleontologia*, v. 7, p. 193–198.
- SINNINGHÉ DAMSTÉ, J.S., EGLINTON, T.I., DE LEEUW, J.W., AND SCHENCK, P.A., 1989, Organic sulphur in macromolecular sedimentary organic matter: I. Structure and origin of sulphur-containing moieties in kerogen, asphaltenes and coal as revealed by flash pyrolysis: *Geochimica et Cosmochimica Acta*, v. 53, p. 873–889.
- SINNINGHÉ DAMSTÉ, J.S., IRENE, W., RIJSTRA, C., DE LEEUW, J.W., AND SCHENCK, P.A., 1988, Origin of organic sulphur compounds and sulphur-containing high molecular weight substances in sediments and immature crude oils: *Organic Geochemistry*, v. 13, p. 593–606.
- STEFFEN, D., AND GORIN, G., 1993, Palynofacies of the Upper Tithonian-Berriasian deep-sea carbonates in the Vocontian Trough (SE France): *Bulletin des Centres de Recherche Exploration-Production Elf-Aquitaine*, v. 17, p. 235–247.
- TAYLOR, T.N., 1999, The ultrastructure of fossil cuticle, in *Fossil Plants and Spores*: Modern Techniques, Jones, T.P., and Rowe, N.P., eds., Geological Society of London, p. 113–115.
- TEGELAAR, E.W., DE LEEUW, J.W., DERENNE, S., AND LARGEAU, C., 1989, A reappraisal of kerogen formation: *Geochimica et Cosmochimica Acta*, v. 53, p. 3103–3106.
- TISSOT, B.P., AND WELTE, D.H., 1984, *Petroleum Formation Occurrence*: Berlin, Springer-Verlag, 699 p.
- TRIBOILLARD, N., TRICHET, J., DEFARGE, C., AND TRENTESAUX, A., 1999, Jurassic lagoonal environments and quasi-abiotic platy limestone accumulation: microbial interventions: *Sedimentology*, v. 46, p. 1183–1197.
- VASCONCELOS, C.O., 1994, Modern dolomite precipitation and diagenesis in a coastal mixed water system (Lagoa Vermelha, Brazil): a microbial model for dolomite formation under anoxic conditions: PhD Thesis, Eidgenössische Technische Hochschule: Zürich.

Received 25 June 2007; accepted 27 April 2008.